Exponential Attenuation of Through-Bond Transmission in a Polyene: Theory and Potential Realizations

Yuta Tsuji,[†] Ramis Movassagh,[‡] Supriyo Datta,[§] and Roald Hoffmann*,[†]

[†]Department of Chemistry and Chemical Biology, Cornell University, Baker Laboratory, Ithaca, New York 14853, United States, [‡]Department of Mathematics, Massachusetts Institute of Technology, Building E18, 77 Massachusetts Avenue, Cambridge, Massachusetts 02139-4307, United States, and [§]School of Electrical and Computer Engineering, Purdue University, Electrical Engineering Building, 465 Northwestern Avenue, West Lafayette, Indiana 47907-2035, United States

ABSTRACT An exponential falloff with separation of electron transfer and transport through molecular wires is observed and has attracted theoretical attention. In this study, the attenuation of transmission in linear and cyclic polyenes is related to bond alternation. The explicit form of the zeroth Green's function in a Hückel model for bond-alternated polyenes leads to an analytical expression of the conductance decay factor β. The β values calculated from our model (β_{CN} values, per repeat unit of double and single bond) range from 0.28 to 0.37, based on carotenoid crystal structures. These theoretical β values are slightly smaller than experimental values. The difference can be assigned to the effect of anchoring groups, which are not included in our model. A local transmission analysis for cyclic polyenes, and for [14]annulene in particular, shows that bond alternation affects dramatically not only the falloff behavior but also the choice of a transmission pathway by electrons. Transmission follows a well-demarcated system of π bonds, even when there is a shorter-distance path with roughly the same kind of "electronic matter" intervening.

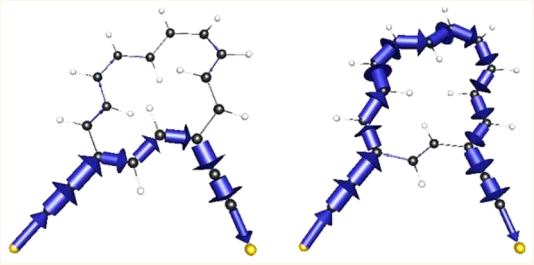

KEYWORDS: molecular transmission · exponential falloff · bond alternation · annulenes

Tunable molecular wires that mediate electronic communication,[1] energy transfer,[2] electron transfer,[3] hole transfer,[4] and charge transport[5] have been a gleam in the eye of theoreticians and experimentalists in our community, especially in molecular electronics.[6] The intimate relationship between the above-named processes has been pointed out.[7,8] It would seem that such mediation might be most effectively achieved through organic π-electron systems, whose electrons are known to be delocalized and mobile. Hence, much effort has been directed over the past three decades to the design and synthesis of π-conjugated molecular wires.[9]

Controlling conductance and current flow through π-conjugated molecular wires is a persistent challenge for molecular electronics. A molecular wire with low (as a function of distance) decay is desirable. From another viewpoint, a donor–bridge–acceptor system with low attenuation of transmission of energy and electrons is indispensable for the construction of biomimetic artificial photosynthetic systems, as well as for understanding many biological and chemical systems.[10] This is the reason for much interest in the distance-dependent attenuation of electron transfer and transport.[11–13]

We construct in this paper a piecewise new perspective on decay and attenuation of transmission through π-electron systems.

RESULTS AND DISCUSSION

Exponential Falloff. Studies on distance-dependent attenuation probably began with examination of tunneling of a particle through a rectangular potential energy barrier by Gamow.[14] The tunneling probability of a particle with mass m through a rectangular potential energy barrier with a height of ΔE and a width of d may be written as follows:

$$\tau \propto \exp(-\beta_{Gamow} d) \qquad (1)$$

* Address correspndence to rh34@cornell.edu.

Received for review July 24, 2015 and accepted September 21, 2015.

Published online September 21, 2015
10.1021/acsnano.5b04615

© 2015 American Chemical Society

where

$$\beta_{\text{Gamow}} = \frac{2\sqrt{2m\Delta E}}{\hbar} \quad (2)$$

Here ΔE is assumed to be independent of d. Equation 2 shows a simple relation between the distance decay constant β and the tunneling barrier height. The decay constant reflects the degree of decrease in the wave function through the potential barrier. This relation can be used to estimate an effective barrier height for electron transfer through various molecules, based on the experimentally measured β values.[3]

Exponentially distance-dependent falloff has been found in the rate constants of coherent off-resonant electron (or hole) transfer phenomena, which are induced by the superexchange mechanism (single-step tunneling).[15] The distance dependence of the electron transfer rate constant is described as follows:[16]

$$k_{\text{ET}} = k_0 \exp(-\beta_{\text{ET}} R_{\text{DA}}) \quad (3)$$

where k_0 is a kinetic prefactor. In the many donor–acceptor systems studied, R_{DA} can be defined as the donor–acceptor center-to-center distance. Equation 3 is empirical and comes from early tunneling calculations. k_{ET} values reflect the rate of charge separation and recombination, which are important properties in the design of efficient photovoltaic devices.[16,17] β_{ET} values, which are regarded as the intrinsic electronic properties of molecular bridges, have been determined experimentally and theoretically for many molecular bridges, for example, proteins,[18,19] DNA,[4,20] saturated hydrocarbons,[21,22] and linear π-conjugated oligomers including oligovinylene (oligoene),[23,24] oligoethenylene (oligoyne),[23,25,26] paraphenylene,[27,28] oligofluorene,[29] oligo(phenylenevinylene),[30] and oligo(phenyleneethynylene).[31,32] The smaller β_{ET} is, the more rapidly and efficiently electron transfer reactions can occur. π-Conjugated oligomers have smaller β_{ET} than proteins, DNA, and saturated hydrocarbons, and hence they are efficient mediators of charge transfer. Oligo(phenylenevinylene) is reported to have the smallest β_{ET} value of 0.01 Å^{-1}.[30]

The semiclassical expression for electron transfer reactions formulated by Marcus[33] provides the basis for relating the rate constant k_{ET} to the electronic coupling H_{DA} and thermodynamic parameters as follows:

$$k_{\text{ET}} = \sqrt{\frac{4\pi^3}{h^2\lambda k_{\text{B}}T}}\, {H_{\text{DA}}}^2 \exp\left\{-\frac{(\Delta G^{\circ} + \lambda)^2}{4\lambda k_{\text{B}}T}\right\} \quad (4)$$

where ΔG^0 is the standard free-energy change for the electron transfer reaction, which is the driving force arising from the difference in the oxidation potentials of the donor and acceptor, and λ is the reorganization energy, which is required for the nuclear rearrangement accompanied by electron transfer. H_{DA} describes the probability of electron tunneling from the donor to acceptor through the bridge. Although ΔG^0 and λ may vary as a function of donor–acceptor separation, it is frequently assumed that H_{DA} plays the dominant role and the distance dependence of k_{ET} originates in large part from H_{DA}.[3] The distance dependence of H_{DA} can be expressed as follows:[2]

$$H_{\text{DA}} = H_{\text{DA}}^0 \exp\left(-\frac{\beta_{\text{EC}}}{2} R_{\text{DA}}\right) \quad (5)$$

where H_{DA}^0 is the electronic coupling at contact distance and β_{EC} is the distance decay constant of the electronic coupling. If the dependence of ΔG^0 and λ on the distance is small, it is possible to assume that $\beta_{\text{EC}} = \beta_{\text{ET}}$.

McConnell[34] used perturbation theory to derive a formula describing H_{DA} in a system in which a covalent bridge composed of N identical repeating units intervenes between the donor and acceptor. McConnell's formula is written as follows:

$$H_{\text{DA}} = \frac{H_{\text{DB}} H_{\text{BA}}}{\Delta\varepsilon}\left(\frac{H_{\text{BB}}}{\Delta\varepsilon}\right)^{N-1} \quad (6)$$

where H_{DB} is the coupling between the donor and the first bridging unit, H_{BA} is that between the last bridging unit and the acceptor, H_{BB} is that between adjacent bridging units, and $\Delta\varepsilon$ is the tunneling energy gap, which is defined as the energy difference between electron (hole) states on the donor (acceptor) and those on the bridge. Here it is assumed that $H_{\text{BB}} \ll \Delta\varepsilon$. McConnell's model describes through-bond donor–acceptor interaction mediated by N identical bridging units.

Comparison between eqs 5 and 6 leads to an expression of β_{EC} in terms of H_{BB} and $\Delta\varepsilon$ as follows:[2]

$$\beta_{\text{EC}} = -\frac{2}{R_0}\ln\left(\frac{H_{\text{BB}}}{\Delta\varepsilon}\right) \quad (7)$$

where R_0 is the length of one repeating unit. R_{DA} is assumed to be linearly proportional to N, *i.e.*, $R_{\text{DA}} \approx NR_0$. It is worth noting that β_{EC} is not a bridge-specific parameter, because $\Delta\varepsilon$ depends on both bridge and donor or acceptor.

McConnell's model has been developed by Evenson and Karplus, based on the Green's function of the bridge.[35] They provided a numerical technique for computing H_{DA}. Reimers and Hush have provided extensions of the McConnell's model, which allow the bridge to be described using two different intersite couplings instead of the single parameter H_{BB}.[36,37] This modified model is appropriate for coupling through a π system containing alternating single and double bonds, as well as a σ system, where carbon valence orbitals are represented using sp^3 hybrids and there is a strong coupling forming a σ bond between the

orbitals on adjacent atoms and a weak coupling between orbitals on the same atom.

Recent dramatic advances in the fabrication technique of electrode−molecule−electrode junctions, for example, scanning probe microscopy, mechanical break junctions, electromigration break junctions, and self-assembly of nanostructures,[38] allow us access to the distance-dependent falloff of molecular conductance. In the coherent off-resonant tunneling transport regime, the conductance g shows an exponential falloff behavior with respect to the transport distance L, which can be defined as a distance between two electrodes,[39] between two anchor atoms,[40] or between terminal carbon atoms,[41] as follows:[13]

$$g = g_0 \exp(-\beta_C L) \tag{8}$$

where g_0 is a constant prefactor that depends on the coupling between the molecular wire and electrode and β_C is the conductance decay constant. Just like eq 3, eq 8 is also empirical and comes from early tunneling calculations.

So far, β_C values have been determined experimentally and theoretically in many molecules, for example, alkanes,[42,43] π-stacked materials,[44,45] metal-ion clusters,[46] extended metal atom chains,[47] and π-conjugated oligomers including oligoenes,[48,49] oligoynes,[50,51] oligoacenes,[52,53] oligothiophenes,[54] oligoporphyrins,[55] oligophenylenes,[56,57] and graphene nanoribbons,[58] combined with various end groups[51] and electrode materials.[59] Although the reported β_C values depend on the experimental and theoretical methodologies to a certain degree,[12] π-conjugated systems generally have smaller β_C values (around 0.2−0.6 Å^{-1}) than σ systems (around 0.6−1.0 Å^{-1}).[60] An extremely small β_C value of 0.006 Å^{-1} has been reported for extended viologen molecules,[61] and even a negative β_C value of −0.117 Å^{-1} has been predicted for graphene nanosheets.[62]

The exponential conductance decay of eq 8 can be rewritten in terms of the number of repeating units in the molecular wires as follows:

$$g = g_0 \exp(-\beta_{CN} N) \tag{9}$$

N is the number of repeat units, for example the number of methylene groups for alkanes (β_{CN} = 1.1/methylene),[63] that of double bonds for oligoenes (β_{CN} = 0.556 or 0.43/double bond),[48,49] and that of benzene rings for phenylenes (β_{CN} = 1.7/benzene ring).[64] Using the length of one repeating unit R_0, β_{CN} can be converted to β_C, as follows:

$$\beta_C = \frac{\beta_{CN}}{R_0} \tag{10}$$

There are a few derivations of β_C and β_{CN}. Onipko and co-workers developed an exactly solvable analytical model that covers conjugated oligomers on the basis of the Landauer approach and Green's function technique.[65] If $\beta_{CN}N \gg 1$, the decay constant can be written as follows:

$$\beta_{CN} = 2 \ln|| f(E_F)|/2 + \sqrt{[f(E_F)/2]^2 - 1}| \tag{11}$$

where $f(E)$ is a function determined by the monomer Green's functions.

Joachim and Magoga[66] employed the calculation of the complex-band structure proposed by Kohn,[67] where the electronic band structure of the periodic extension of a finite-length molecular wire can be obtained by solving the Schrödinger equation with a complex-valued wave vector. They showed that β_C depends on the energy-dependent effective mass $m^*(E)$ as well as the HOMO−LUMO gap χ for the molecular wire as follows:

$$\beta_C = \sqrt{\frac{2m^*(E_F)}{\hbar^2}\frac{(E_F - E_{HOMO})(E_{LUMO} - E_F)}{\chi}} \tag{12}$$

Engelkes, Beebe, and Frisbie[63] derived an analytical expression for β_{CN} using a model for a molecular junction composed of an N-site carbon chain, where each site has a site energy E_C and an overlap energy with its neighboring site $V_{C,C}$. Their expression for β_{CN} can be written as follows:

$$\beta_{CN} = 2 \ln\left(\frac{E_C - E_F}{V_{C,C}}\right) \tag{13}$$

If $E_C - E_F$ is regarded as the tunneling energy gap $\Delta\varepsilon$, eq 13 can be reduced to McConnell's formula eq 7. This equation predicts that β_{CN} should depend on the Fermi level and therefore the electrode work function and applied bias. However, experiments by Engelkes *et al.* indicated that the latter effect is not large.[63]

More recently, Stuyver and co-workers have provided an elegant method based on a relation between the zeroth-order Green's function, the Pauling bond order, and the number of Kekulé structures, deriving an analytical expression for exponential decay in transmission for oligo(*p*-phenylene).[68]

We believe that it would be useful to connect the decay constant to the geometrical features of molecular wires, such as bond lengths and dihedral angles. Here we derive an expression for the decay constant β_{CN} based on the zeroth-order Green's function in the Hückel model for linear polyenes with alternating single and double bonds, and we compare the derived β values with experimental results. The alternation is critical to the attenuation. We also discuss electron transport properties through cyclic polyenes with bond alternation.

Derivation of an Expression for β for Polyenes with Bond Alternation. In the Hückel Hamiltonian matrix for a polyene chain consisting of uniformly spaced carbons, all resonance integrals are set equal. To avoid confusion with the prevalent use of β for a decay constant,

we use here t for the resonance integral instead of the standard notation β. t for transfer integral is anyway the standard notation of tight-binding theory in solid-state physics. The Hückel Hamiltonian matrix for a linear polyene without bond alternation takes on the form of a bordered matrix as follows:

$$\mathbf{H} = \begin{bmatrix} 0 & 1 & & & & & \\ 1 & 0 & 1 & & & & \\ & 1 & 0 & \ddots & & & \\ & & \ddots & \ddots & 1 & & \\ & & & 1 & 0 & 1 & \\ & & & & 1 & 0 & \end{bmatrix} \quad (14)$$

Since we use energy units of t (<0), which is the resonance integral between adjacent 2pπ orbitals in a benzene ring, the nearest neighbor interactions are replaced by 1. The diagonal terms, the Coulomb integrals typically labeled α, are set to an energy zero.

To express the Hückel Hamiltonian matrix for a linear polyene with bond alternation, the Hamiltonian matrix shown in eq 14 can be modified as follows:

$$\mathbf{H} = \begin{bmatrix} 0 & t_D & & & & & \\ t_D & 0 & t_S & & & & \\ & t_S & 0 & \ddots & & & \\ & & \ddots & \ddots & t_S & & \\ & & & t_S & 0 & t_D & \\ & & & & t_D & 0 & \end{bmatrix} \quad (15)$$

where t_S and t_D are the resonance integrals for single and double bonds, respectively.

If we consider molecules weakly coupled to the contacts such that the conduction properties can be understood from the zeroth-order Green's function at the Fermi energy, then

$$\mathbf{G}(E_F) \approx \mathbf{G}^{(0)}(E_F) = [(E_F + i\eta)\mathbf{I} - \mathbf{H}]^{-1} \quad (16)$$

where η is an infinitesimal positive number and $\mathbf{I}$ is the unit matrix. Here we restrict our attention to the half-filled π bands of linear chains and cyclic molecules. It is reasonable to assume that the Fermi level lies at the midpoint between the highest occupied band and the lowest unoccupied band (if there is no significant charge transfer between the molecule and electrode).[69,70] In the Hückel approximation, such a definition of the Fermi level leads to the situation where both the Fermi level and the Coulomb integral may be set to be the energy zero.[71]

In this paper we confine our discussion to even-numbered neutral carbon chains or cycles so that the Fermi level cannot coincide with any of the eigenenergies of $\mathbf{H}$, which allows us to neglect the infinitesimal η. Under the assumptions of $E_F = 0$ and $\eta \to 0$, we have what we call the zeroth-order Green's function:

$$G(r, s) \equiv [\mathbf{G}^{(0)}(E_F = 0)]_{rs} \approx [-\mathbf{H}^{-1}]_{rs} \quad (17)$$

On the basis of the methodology described elsewhere,[72] when the Hamiltonian matrix for a linear polyene with bond alternation, namely, eq 15, is substituted into the Hamiltonian in eq 17, the matrix elements of the zeroth-order Green's function are derived in ref 71:

$$G(r, s) = \frac{(-1)^{(r+s-1)/2}}{4} \frac{1}{t_D} \left(\frac{t_S}{t_D}\right)^{(s-r-1)/2} [1 - (-1)^r][1 + (-1)^s] \quad (18)$$

where $r \le s$. Many $G(r, s)$ values are zero, examples of quantum interference. For instance all (r, s) = (odd, odd) and (even, even) are zero, as are $G(r, s)$ with r even, $r < s$.

Let us consider a two-probe molecular junction, in which two specific atoms denoted by r and s in the molecule are connected to the left and right electrodes, respectively. The coupling strength between the molecule and electrodes can be described by the nonzero elements of the broadening function matrices for the left and right electrodes, *viz.*, γ_L and γ_R. The low-bias conductance through such a molecular junction can be approximated by using the zeroth-order Green's function, as follows:[70]

$$g = \frac{2e^2}{h} T(E_F) \approx \frac{2e^2}{h} \gamma_L \gamma_R |G(r, s)|^2 \quad (19)$$

where $2e^2/h$ is the quantum of conductance and T is the transmission probability.

Let us consider a molecular junction composed of a polyene chain with N double bonds, where the left and right electrodes are connected to the carbon atoms at both ends, as shown in Scheme 1. In this situation $r = 1$ and $s = 2N$. Using eqs 18 and 19, we can obtain the conductance through a polyene as a function of N:

$$g = \frac{2e^2}{h} \gamma_L \gamma_R \frac{1}{t_S^2} \left(\frac{t_S}{t_D}\right)^{2N} \quad (20)$$

Comparison of the natural logarithms of eqs 9 and 20 in terms of N leads to an expression for the decay

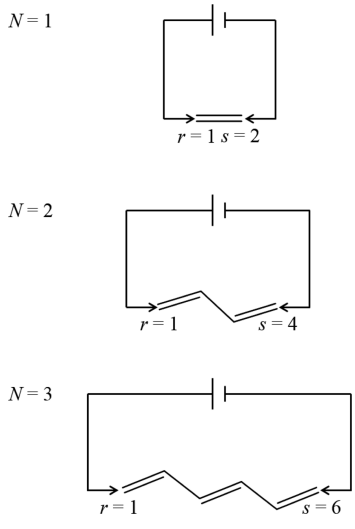

Scheme 1. Schematic representation of a molecular junction comprising a polyene chain with N double bonds, whose ends are connected to the left and right electrodes.

constant β_{CN} (per molecular repeat unit, here a double bond and a single bond) as follows:

$$\beta_{CN} = -2 \ln\left(\frac{t_S}{t_D}\right) \quad (21)$$

This equation implies that the conductance decay constant should depend on the degree of bond alternation, *i.e.*, the ratio of double bond to single bond resonance or transfer integrals. The dependence *n* has been investigated with a numerical approach using complex band structure calculation[73] and an experiment using a cross-wire tunnel junction.[74] Recently Lambert and co-workers also derived an analytical expression for the decay constant without using the Green's function formalism.[75]

Equation 21 is plotted in Figure 1. If $t_D > t_S$, which is a normal situation for polyenes, $\beta_{CN} > 0$, which means that the conductance keeps exponentially decreasing as the number of double bonds between the left and right electrodes gets larger, as observed in experiments[48,49] earlier. If $t_D = t_S$, which is the case of bond-equalized polyenes, $\beta_{CN} = 0$, which means that the conductance should be independent of the number of double bonds between the left and right electrodes. This is, of course, a desirable situation for molecular wires. But the ubiquitous Peierls distortion,[76] first applied to polyenes by Salem and Longuet-Higgins,[77] does not allow this. However, with application of an external electric field,[78] it might be possible to minimize bond alternation and hence reach nearly zero β_{CN} values, as $t_S/t_D \rightarrow 1$.

The case of $t_D < t_S$ is very interesting because it implies $\beta_{CN} < 0$, which means that the conductance would increase exponentially as the number of double bonds between the left and right electrodes gets larger. This sounds counterintuitive, and indeed $t_D < t_S$ is just chemically unreasonable in the ground state of a molecule. But it might be achievable in a low-lying excited state.[79] Actually, Lindsay and co-workers have reported the measurement of conductance through a light-induced excited state of a porphyrin-C_{60} dyad molecule.[80] In the SI, we explore the unphysical assumption of $t_D < t_S$ in a detailed calculation.

Comparison between Theoretical and Experimental β Values. To evaluate β_{CN}, the ratio between the resonance integrals for the single and double bonds is required. This ratio can be calculated by using Mulliken's formula[81] as follows:

$$\frac{t_S}{t_D} = \frac{S_S}{S_D} \quad (22)$$

where S_S and S_D are the overlap integrals between adjacent 2pπ orbitals in single and double bonds, respectively. These overlap integrals can be calculated explicitly.[82] If the $2p_z$ orbital is a single carbon Slater function, $z \exp(-pr)$ (unnormalized), where $p = 3.072R$ and R is the separation in Å of the interacting carbon nuclei, then the $2p_z$–$2p_z$ π-type overlap integral is

$$S = e^{-p}\left[1 + p + \frac{2}{5}p^2 + \frac{1}{15}p^3\right] \quad (23)$$

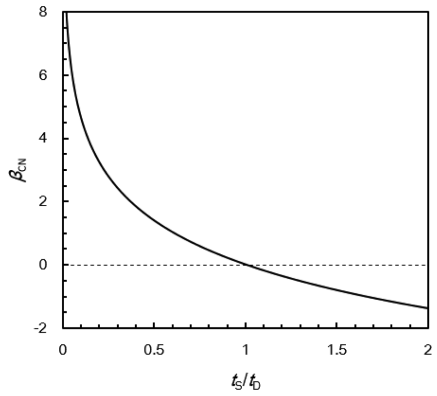

Figure 1. β_{CN} is plotted as a function of t_S/t_D based on eq 21.

We have checked the crystal structures of various carotenoid polyenes,[83−86] which have the all-*trans* configuration. We then calculated the average bond length of the single and double bonds for each carotenoid polyene.[87] From the average bond lengths, the overlap integrals and then t_S/t_D are calculated. We have found that the value of t_S/t_D for carotenoid polyenes is in a range from 0.83 to 0.87, which can be converted into β_{CN} values that range from 0.28 to 0.37.

He *et al*. measured the conductance of a series of carotenoid polyenes terminated with a benzene ring coupled to a thiol *via* a methylene linker using a scanning tunneling microscope (STM).[48] The shortest carotenoid polyene investigated in their experiment is shown in Figure 2a. They reported a β_{CN} value of 0.556 ± 0.09. Visoly-Fisher *et al*. measured the conductance of a series of carotenoid polyenes terminated with a pyridine linker using an STM.[49] The shortest carotenoid polyene investigated in their experiment is shown in Figure 2b. They reported a β_{CN} value of 0.43 ± 0.07. They attributed the variation of the β_{CN} values to the effect of the end groups on the alignment of molecular states with the Fermi level of the electrode.

Recently Dell *et al*. measured the conductance of a series of molecules that contain thiophene-1,1-dioxide (TDO).[88] Since the lone pairs of sulfur in the thiophene unit are engaged in bonding to oxygen, the TDO moiety provides an oligoene-like backbone. However, this is not the all-*trans* configuration seen in the carotenoids. Their β_{CN} value is 0.52, which lies midway between the values obtained by He *et al*. and Visoly-Fisher *et al*.

The β_{CN} values obtained from the experiments by He *et al*., Visoly-Fisher *et al*., and Dell *et al*. are larger than our expected value; that is, the conductance falls off faster than we predict. The most significant

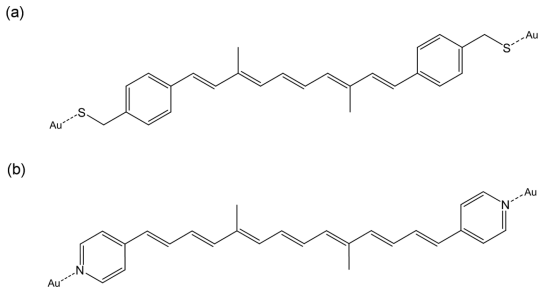

Figure 2. Example for the structure of carotenoid polyenes measured by (a) He *et al*. and (b) Visoly-Fisher *et al*.

difference in the situation between our model and the experiments is the anchoring group that connects the molecule to the electrode. In our model, as shown in Scheme 1, no anchor groups are taken into account. The anchoring groups make real differences, such as the shift of the Fermi level and introducing additional tunneling barriers. Plausible considerations that may bridge the gap between our model and experiments are presented in detail in the Supporting Information (SI).

Conductance in Cyclic Polyenes with Bond Alternation. Let us investigate conductance in cyclic polyenes with bond alternation. To express the Hückel Hamiltonian matrix for cyclic polyenes with bond alternation, the Hamiltonian matrix shown in eq 15 can be modified as follows:

$$\mathbf{H} = \begin{bmatrix} 0 & t_D & & & & t_S \\ t_D & 0 & t_S & & & \\ & t_S & 0 & \ddots & & \\ & & \ddots & \ddots & t_S & \\ & & & t_S & 0 & t_D \\ t_S & & & & t_D & 0 \end{bmatrix} \quad (24)$$

We have recently obtained an analytical expression for the entries of the zeroth-order Green's function for this Hamiltonian matrix. The derivation will be discussed elsewhere;[72] here we give the result:

$$G(r,s) = -\frac{1}{4}\left\{\frac{(-t_S/t_D)^{(M+r-s-1)/2}}{t_D[1-(-t_S/t_D)^{M/2}]}[1+(-1)^r][1-(-1)^s] + \frac{(-t_D/t_S)^{(M+r-s-1)/2}}{t_S[1-(-t_D/t_S)^{M/2}]}[1-(-1)^r][1+(-1)^s]\right\} \quad (25)$$

where $r \le s$ and M is the total number of carbon atoms.

For cyclic polyenes containing $4n+2$ carbon atoms, namely, [$4n+2$]annulenes, Longuet-Higgins and Salem theoretically predicted that if n is less than 8, the symmetrical structure should be preferred, but that for greater values of n bond alternation should set in.[89] However, a combined theoretical and experimental study by Schaefer, Schleyer, and co-workers showed that the crossover point between bond-equalized and bond-alternated structures occurs much earlier, at around $n = 3$ or 4, namely, [14]annulene or [18]annulene.[90] Structural studies of the larger cyclic polyenes are nontrivial; disorder has to be overcome.

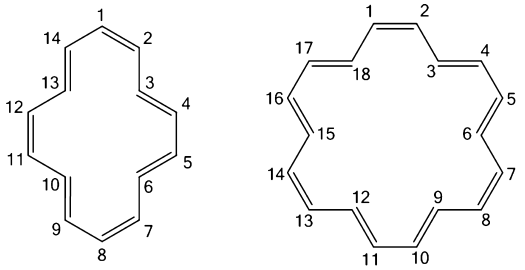

Scheme 2. Bond-alternated representation of [14]annulene and [18]annulene with carbon atom numbering.

Schaefer, Schleyer, and co-workers suggest strongly that the structures be reinvestigated.

Representations of [14]annulene and [18]annulene with alternating bonds are shown in Scheme 2 (effectively one Kekulé structure) with carbon atom numbering.

Schaefer, Schleyer, and co-workers predicted that in the geometries of [14]annulene and [18]annulene the average lengths of the single and double bonds are 1.44 and 1.35 Å, respectively, for both [14]annulene and [18]annulene. The resonance integrals for the single and double bonds of these molecules are estimated (by the procedure detailed above) to be 0.93 and 1.09, respectively, using the resonance integral for the CC bond length of 1.40 Å in benzene as a reference. Using these values for t_S and t_D in eqs 24 and 25, the zeroth-order Green's function matrices for [14]annulene and [18]annulene are calculated. The first rows of the zeroth-order Green's function matrices for [14]annulene and [18]annulene are [0, −0.69, 0, 0.59, 0, −0.50, 0, 0.43, 0, −0.37, 0, 0.31, 0, −0.27] and [0, −0.74, 0, 0.63, 0, −0.54, 0, 0.46, 0, −0.39, 0, 0.33, 0, −0.29, 0, 0.24, 0, −0.21], respectively. If there were no bond alternation, all nonzero elements would be +0.5 or −0.5.[71]

In Figure 3a and b are plotted the nonzero elements in the first row of the zeroth-order Green's function, namely, $G(1, s)$, and their squares (in parentheses). The latter should reflect the conductance between the C1 atom and another carbon atom. In Figure 4 the absolute squared values of $G(1, s)$ are plotted logarithmically as a function of the number of intervening double bonds N between the first and second electrodes. Importantly, the "distance" N here is measured "the polyene way", around $1 \le N \le 7$ for [14]annulene and $1 \le N \le 9$ for [18]annulene.

Figure 4 shows that the conductance through cyclic polyenes with bond alternation also follows an exponential falloff behavior. The inclination of the approximation lines for [14]annulene and [18]annulene leads to a β_{CN} value of 0.32, which is fully consistent with the β_{CN} value calculated from eq 21, although this equation is derived from a model for linear polyenes with bond alternation.

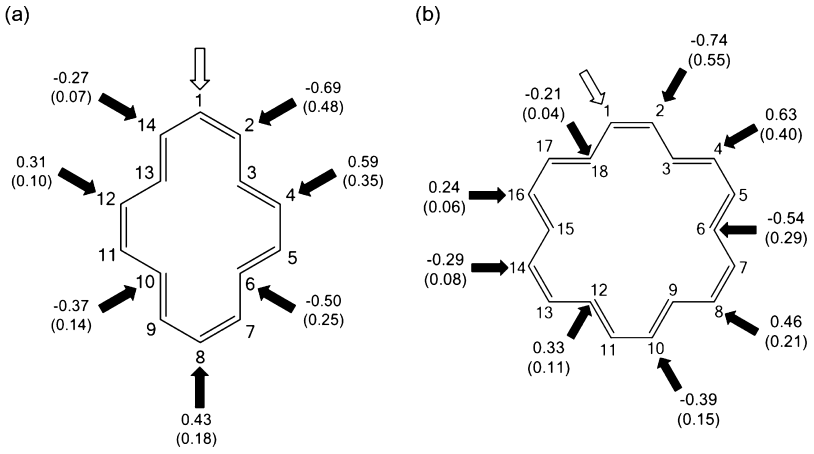

Figure 3. Values of the zeroth-order Green's function $G(1, s)$ for (a) [14]annulene and (b) [18]annulene. The white arrow denotes the attachment position of the first electrode, and the black arrow marks conceivable attachment positions of the second electrode. The numbers in parentheses are the absolute squared values of $G(1, s)$.

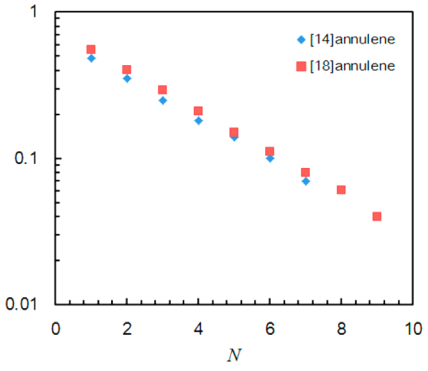

Figure 4. Absolute squared values of $G(1, s)$ are plotted *versus* the number of double bonds N between the first and second electrodes along "the polyene way" beginning with the double bonds, which corresponds to $s/2$.

Let us use the analytical expression eq 25 to rationalize the above-mentioned numerical results. When $r = 1$ and s is even, the first term of eq 25 is zero and the leftover term is

$$G(1, s) = \frac{(-t_D/t_S)^{(M-s)/2}}{t_S[1-(-t_D/t_S)^{M/2}]} \quad (26)$$

and its absolute square is

$$|G(1, s)|^2 = \frac{(t_D/t_S)^M}{t_S^2[1-(-t_D/t_S)^{M/2}]^2}(t_S/t_D)^s \quad (27)$$

Since M is the total number of carbon atoms included in the ring, which is fixed, only $(t_S/t_D)^s$ is variable and the conductance is proportional to $(t_S/t_D)^s$. s corresponds to $2N$, where N is the number of intervening double bonds between the first and second electrodes. Thence, the conductance through the cyclic polyene with bond alternation can be written as follows:

$$g = \frac{2e^2}{h}\gamma_L\gamma_R\frac{(t_D/t_S)^M}{t_S^2[1-(-t_D/t_S)^{M/2}]^2}(t_S/t_D)^{2N} \quad (28)$$

Comparing the natural logarithms of eqs 9 and 28 as a function of N, we arrive at eq 21. Therefore, eq 21 is valid for both linear and cyclic polyenes, within the approximations made.

The Consequences of Bond Alternation. Suppose it were possible to attach electrodes to two neighboring atoms in a cyclic polyene, in particular 1−2 and 1−14 in [14]annulene and 1−2 *versus* 1−18 in [18]annulene. The transmission should go as the Green's function absolute value squared. This would imply a ratio of 1−2 to 1−2N transmission of 6.9 for $N = 7$ and 13.8 for $N = 9$. These are remarkable differences in predicted transmission for a very similar separation in space. A detailed analysis of how the transmission ratio depends on the position of the Fermi level in the electrodes and a specific probing of the calculated transmission spectra for 1−2 and 1−14 connections in [14]annulene are shown in the SI. The significant difference between the 1−2 and 1−14 transmissions can be observed throughout the -0.5β to 0.5β energy window.

The longer the polyene or cyclic polyene is, the larger this ratio is. The limit of the 1−2 connection *versus* 1−M connection in an [M]annulene is analogous to the case of the 1−2 connection *versus* 2−3 connection in butadiene, as shown in Scheme 3, where the absolute squared values of the zeroth-order Green's function for the 1−2 and 2−3 connections are 1 and 0, respectively, if the effect of non-nearest-neighbor couplings[70] and many-body effects[91] are negligible.

The anchoring between the molecule and the metal electrodes is crucial to transport.[92] In thinking of comparing a 1−2 electrode connection with a 1-M one, clearly there is a problem with electrode attachment; steric interference may preclude this experiment. More realistic, we think, would be a comparison of 1−4 *versus* 1−12 connection in [14]annulene. We studied this case in some detail.

Thiol is the most widely used linker to adsorb on a gold surface.[93] In our calculations the thiol groups are

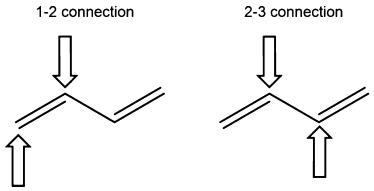

Scheme 3. The 1−2 connection (left) and 2−3 connection (right) of electrodes to butadiene. The electrodes are denoted by arrows.

further linked to [14]annulene by acetylene linkers in order to avoid steric hindrance between the molecule and the electrodes. We began by optimizing the structure of [14]annulenes with the linkers at C1 and C4 atoms and at C1 and C12 atoms with the BHandHLYP functional and 6-311+G(d,p) basis set, as implemented in the Gaussian 09 software.[94] This combination of functional and basis set is suggested by Schaefer, Schleyer, and co-workers.[89] The left and right electrodes are approximated by a Au_9 cluster. The thiol's hydrogen atoms were removed and the clusters were attached in accordance with the methodology shown in a recent study.[95] The adsorption site is the fcc hollow site. The systems investigated are shown in Figure 5.

Single-point DFT calculations were done for the Au_9−molecule−Au_9 structures. The DFT calculations have been carried out with the BHandHLYP functional and LanL2MB basis set, as implemented in the Gaussian 09 software. We adopted a smaller basis set to avoid the problem of ghost transmission and to get a clear picture of local transmission, which will be discussed in the next section; smaller basis functions are more localized on the atoms on which they are centered and therefore are more suitable for the definition of atoms in molecules.[96,97] On the basis of the Fock and overlap matrices obtained from Gaussian 09, electron transport calculations have been done by using the postprocessing tool Artaios.[96,98]

The bond alternation features that are seen in Figure 5 are not significantly different from unsubstituted [14]annulene. The transmission ratio predicted 1−4/1−12 is 0.35/0.10 = 3.5 (see Figure 3). At the Fermi level, which is defined here as the midpoint energy between the HOMO and LUMO of the whole Au_9−molecule−Au_9 structure, the actual calculated transmissions for the optimized structures of Figure 5 are 6.9×10^{-3} and 1.2×10^{-3}, respectively, for a ratio of 5.75. That is quite a large difference, given the very similar metric distances between the electrodes, so clearly seen in Figure 5.

Relation between Bond Alternation and Local Transmission. For another perspective on the effect of bond alternation on transmission we use a local transmission analysis.[99−101] In this method the total transmission can be decomposed into local (atomic) contributions as follows:

$$T(E) = \sum_{A\in L,\, B\in R} T_{AB}(E) \qquad (29)$$

where T_{AB} is the transmission for electrons between centers *A* and *B*. *A* and *B* are usually atoms, which are defined by the basis functions centered on them after a symmetric (Löwdin) orthogonalization. T_{AB} can be calculated on the basis of the Fock and overlap matrices that are the same as those used for the transmission calculations mentioned above.

Local transmission plots are given in Figure 6 to illustrate how the local transmission pattern is changed depending on the bond alternation pattern. This figure shows ever-so-graphically that the main transmission is not through-space but through-π-bonds. 1−4 and 1−12 mean exactly that. In the bond-alternated annulenes the transmissions go "the polyene way" following the alternating double bonds, and there is an attenuation along those paths, naturally greater for the 1−12 path than for the 1−4 one.

For comparison purposes, and prompted by a question to us by Mark Ratner, we considered a 1−4 connection in a bond-equalized [14]annulene, whose structure was optimized under the restriction that all CC bond lengths included in the annulene ring are fixed to 1.4 Å. The calculated transmission probability is not much lower than for the 1−4 case, 6.1×10^{-3}. The local transport contribution picture of this bond-equalized case, Figure 6c, is fascinating: a hybrid of the two bond-localized paths.

That transmission follows a well-demarcated system of π bonds, even when there is a shorter-distance path with roughly the same kind of "electronic matter" intervening, is supported by another study we have carried out, here described only briefly. The system in question is an all-*s-cis* oligoene, sketched in **1** for octatetraene.

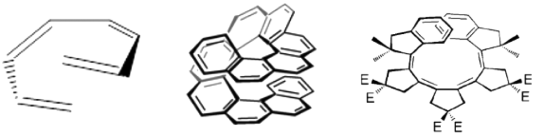

1 **2** **3**

These are not known; of course, they are sterically at a disadvantage relative to their all-*s-trans* conformers. The *s-cis* conformations are frozen in helicenes (exemplified by an 11-helicene, **2**),[102] and, remarkably, compounds in between **1** and **2**, appropriately called "helicenes truncated to a minimum", **3**, have been synthesized.[103]

We have modeled all-*s-cis* hexatriene and octatetraene and studied 1−*n* transmission in these, in work to be reported elsewhere. The 1 and *n* positions emerge relatively close to each other through space, but significantly further apart along the π chain. Dihedral angle changes between π bonds complicate the matter, but the overall theoretical finding (no experiment yet) is of dominant transmission, with falloff, along the π-bond chain.

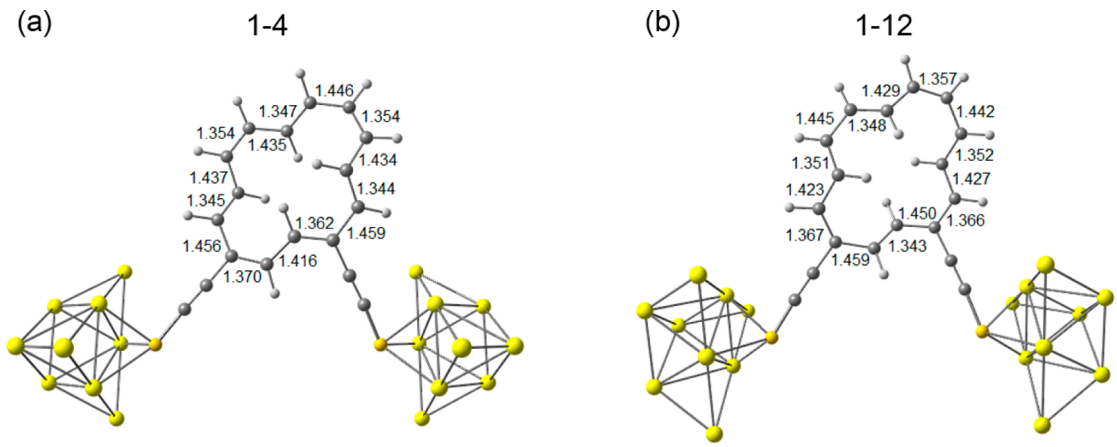

Figure 5. Electrode−molecule−electrode structures for (a) the 1−4 connection and (b) the 1−12 connection of [14]annulene. Selected bond lengths (Å) are shown.

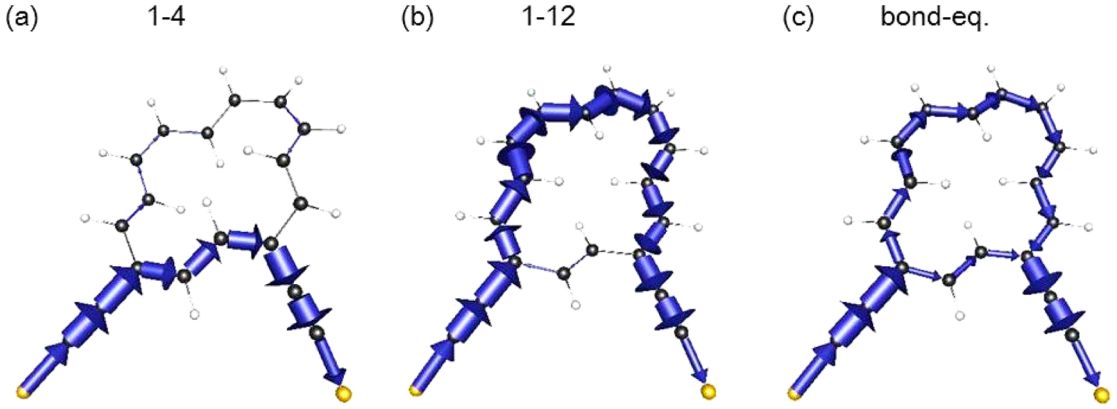

Figure 6. Local transport contributions in (a) the 1−4 and (b) 1−12 connections of the bond-alternated [14]annulene and (c) the 1−4 connection of bond-equalized [14]annulene at the Fermi level. The local transmission contributions are depicted only if above a threshold value of 0.05. The diameter of the arrows represents the value of the local transmission for a pair of atoms.

CONCLUSION

We find that bond alternation plays an essential role in determining transmission through a π system. Exponential falloff of conductance, transmission, or electron transfer is an empirical rule of thumb in the field of molecular electronics. On the basis of a Hückel model for bond-alternated linear polyenes, we derive just such an exponential falloff of conductance with respect to the transport distance. We predict an exponential attenuation factor and compare it with experimental values. The predicted values are smaller than the experimental value; that is, the experimentally measured transmission falls off faster with distance. This discrepancy might be assigned to the effect from the relatively large anchoring groups used in the experiments, which are not included in our model.

We have also investigated the exponential attenuation of conductance in bond-alternated cyclic polyenes, such as [14]annulene and [18]annulene. Bond alternation in cyclic polyenes also results in exponential falloff of conductance. What matters is not the distance through space, but the distance measured along the polyene, though the π bonds. The effect is impressive in size and clearly displayed in local transmission plots. A specific test of the prediction is suggested for 1−4 *versus* 1−12 connections on a [14]annulene skeleton.

Conflict of Interest: The authors declare no competing financial interest.

Acknowledgment. We are grateful to Gemma Solomon and Mark Ratner for their comments and Carmen Herrmann for supplying the ARTAIOS program to us. Y.T. thanks the Japan Society for the Promotion of Science for a JSPS Postdoctoral Fellowship for Research Abroad. R.M. thanks the National Science Foundation through Grants DMS 1312831. Our work at Cornell was supported by the National Science Foundation through Grant CHE-1305872.

Supporting Information Available: The Supporting Information is available free of charge on the ACS Publications website at DOI: 10.1021/acsnano.5b04615.

Details of calculations for the carotenoid polyenes; a possible rationalization for the disagreement between our Hückel model and experiments (PDF)

REFERENCES AND NOTES

1. Herrmann, C.; Elmisz, J. Electronic Communication through Molecular Bridges. *Chem. Commun.* **2013**, *49*, 10456–10458.

2. Eng, M. P.; Albinsson, B. Non-Exponential Distance Dependence of Bridge-Mediated Electronic Coupling. *Angew. Chem., Int. Ed.* **2006**, *45*, 5626–5629.
3. Wenger, O. S. How Donor−Bridge−Acceptor Energetics Influence Electron Tunneling Dynamics and Their Distance Dependences. *Acc. Chem. Res.* **2011**, *44*, 25–35.
4. Giese, B.; Amaudrut, J.; Köhler, A.-K.; Spormann, M.; Wessely, S. Direct Observation of Hole Transfer through DNA by Hopping between Adenine Bases and by Tunneling. *Nature* **2001**, *412*, 318–320.
5. Nitzan, A.; Ratner, M. A. Electron Transport in Molecular Wire Junctions. *Science* **2003**, *300*, 1384–1389.
6. Tao, N. J. Electron transport in molecular junctions. *Nat. Nanotechnol.* **2006**, *1*, 173–181.
7. Kirk, M. L.; Shultz, D. A.; Stasiw, D. E.; Lewis, G. F.; Wang, G.; Brannen, C. L.; Sommer, R. D.; Boyle, P. D. Superexchange Contributions to Distance Dependence of Electron Transfer/Transport: Exchange and Electronic Coupling in Oligo(para-Phenylene)- and Oligo(2,5-Thiophene)-Bridged Donor−Bridge−Acceptor Biradical Complexes. *J. Am. Chem. Soc.* **2013**, *135*, 17144–17154.
8. Nishizawa, S.; Hasegawa, J.; Matsuda, K. Theoretical Investigation of the β Value of the π-Conjugated Molecular Wires by Evaluating Exchange Interaction between Organic Radicals. *J. Phys. Chem. C* **2013**, *117*, 26280–26286.
9. Tour, J. M. Molecular Electronics. Synthesis and Testing of Components. *Acc. Chem. Res.* **2000**, *33*, 791–804.
10. Albinsson, B.; Mårtensson, J. Long-Range Electron and Excitation Energy Transfer in Donor−Bridge−Acceptor Systems. *J. Photochem. Photobiol., C* **2008**, *9*, 138–155.
11. Winkler, J. R.; Gray, H. B. Long-Range Electron Tunneling. *J. Am. Chem. Soc.* **2014**, *136*, 2930–2939.
12. Liu, H.; Wang, N.; Zhao, J.; Guo, Y.; Yin, X.; Boey, F. Y. C.; Zhang, H. Length-Dependent Conductance of Molecular Wires and Contact Resistance in Metal−Molecule−Metal Junctions. *ChemPhysChem* **2008**, *9*, 1416–1424.
13. Khoo, K. H.; Chen, Y.; Li, S.; Quek, S. Y. Length Dependence of Electron Transport through Molecular Wires − a First Principles Perspective. *Phys. Chem. Chem. Phys.* **2015**, *17*, 77–96.
14. Gamow, G. Zur Quantentheorie des Atomkernes. *Eur. Phys. J. A* **1928**, *51*, 204–212.
15. Jortner, J.; Bixon, M.; Langenbacher, T.; Michel-Beyerle, M. E. Charge Transfer and Transport in DNA. *Proc. Natl. Acad. Sci. U. S. A.* **1998**, *95*, 12759–12765.
16. Schubert, C.; Margraf, J. T.; Clark, T.; Guldi, D. M. Molecular Wires − Impact of π-Conjugation and Implementation of Molecular Bottlenecks. *Chem. Soc. Rev.* **2015**, *44*, 988–998.
17. Maggio, E.; Solomon, G. C.; Troisi, A. Exploiting Quantum Interference in Dye Sensitized Solar Cells. *ACS Nano* **2014**, *8*, 409–418.
18. Beratan, D. N.; Betts, J. N.; Onuchic, J. N. Protein Electron Transfer Rates Set by the Bridging Secondary and Tertiary Structure. *Science* **1991**, *252*, 1285–1288.
19. Beratan, D. N.; Onuchic, J. N.; Winkler, J. R.; Gray, H. B. Electron-Tunneling Pathways in Proteins. *Science* **1992**, *258*, 1740.
20. Giese, B. Long-Distance Charge Transport in DNA: The Hopping Mechanism. *Acc. Chem. Res.* **2000**, *33*, 631–636.
21. Johnson, M. D.; Miller, J. R.; Green, N. S.; Closs, G. Distance Dependence of Intramolecular Hole and Electron Transfer in Organic Radical Ions. L. *J. Phys. Chem.* **1989**, *93*, 1173–1176.
22. Paddon-Row, M. N. Investigating Long-Range Electron-Transfer Processes with Rigid, Covalently Linked Donor-(Norbornylogous Bridge)-Acceptor Systems. *Acc. Chem. Res.* **1994**, *27*, 18–25.
23. Benniston, A. C.; Goulle, V.; Harriman, A.; Lehn, J.-M.; Marczinke, B. Electron Delocalization in Polyene-Bridged Binuclear Complexes. *J. Phys. Chem.* **1994**, *98*, 7798–7804.
24. Osuka, A.; Tanabe, N.; Kawabata, S.; Yamazaki, I.; Nishimura, Y. Synthesis and Intramolecular Electron- and Energy-Transfer Reactions of Polyyne- or Polyene-Bridged Diporphyrins. *J. Org. Chem.* **1995**, *60*, 7177–7185.
25. Grosshenny, V.; Harriman, A.; Ziessel, R. Towards the Development of Molecular Wires: Electron Localization, Exchange, and Transfer in Alkyne-Bridged Multinuclear Complexes. *Angew. Chem., Int. Ed. Engl.* **1996**, *34*, 2705–2708.
26. Vail, S. A.; Krawczuk, P. J.; Guldi, D. M.; Palkar, A.; Echegoyen, L.; Tomé, J. P. C.; Fazio, M. A.; Schuster, D. I. Energy and Electron Transfer in Polyacetylene-Linked Zinc−Porphyrin−[60]Fullerene Molecular Wires. *Chem. - Eur. J.* **2005**, *11*, 3375–3388.
27. Barigelletti, F.; Flamigni, L.; Guardigli, M.; Juris, A.; Beley, M.; Chodorowski-Kimmes, S.; Collin, J. P.; Sauvage, J. P. Energy Transfer in Rigid Ru(II)/Os(II) Dinuclear Complexes with Biscyclometalating Bridging Ligands Containing a Variable Number of Phenylene Units. *Inorg. Chem.* **1996**, *35*, 136–142.
28. Schlicke, B.; Belser, P.; De Cola, L.; Sabbioni, E.; Balzani, V. Photonic Wires of Nanometric Dimensions. Electronic Energy Transfer in Rigid Rodlike Ru(bpy)32+-(ph)n-Os(bpy)32+ Compounds (ph = 1,4-Phenylene; n = 3, 5, 7). *J. Am. Chem. Soc.* **1999**, *121*, 4207–4214.
29. Wielopolski, M.; Rojas, G.; van der Pol, C.; Brinkhaus, L.; Katsukis, G.; Bryce, M. R.; Clark, T.; Guldi, D. M. Control over Charge Transfer through Molecular Wires by Temperature and Chemical Structure Modifications. *ACS Nano* **2010**, *4*, 6449–6462.
30. Davis, W. B.; Svec, W. A.; Ratner, M. A.; Wasielewski, M. R. Molecular-Wire Behaviour in p-Phenylenevinylene Oligomers. *Nature* **1998**, *396*, 60–63.
31. Pettersson, K.; Kyrychenko, A.; Ronnow, E.; Ljungdahl, T.; Martensson, J.; Albinsson, B. Singlet Energy Transfer in Porphyrin-Based Donor−Bridge−Acceptor Systems: Interaction between Bridge Length and Bridge Energy. *J. Phys. Chem. A* **2006**, *110*, 310–318.
32. Pettersson, K.; Wiberg, J.; Ljungdahl, T.; Martensson, J.; Albinsson, B. Interplay between Barrier Width and Height in Electron Tunneling: Photoinduced Electron Transfer in Porphyrin-Based Donor−Bridge−Acceptor Systems. *J. Phys. Chem. A* **2006**, *110*, 319–326.
33. Marcus, R. A.; Sutin, N. Electron Transfers in Chemistry and Biology. *Biochim. Biophys. Acta, Rev. Bioenerg.* **1985**, *811*, 265–322.
34. McConnell, H. M. Intramolecular Charge Transfer in Aromatic Free Radicals. *J. Chem. Phys.* **1961**, *35*, 508–515.
35. Evenson, J. W.; Karplus, M. Effective Coupling in Bridged Electron Transfer Molecules: Computational Formulation and Examples. *J. Chem. Phys.* **1992**, *96*, 5272–5278.
36. Reimers, J. R.; Hush, N. S. Electron Transfer and Energy Transfer through Bridged Systems III. Tight-Binding Linkages with Zero or Non-Zero Asymptotic Band Gap. *J. Photochem. Photobiol., A* **1994**, *82*, 31–46.
37. Reimers, J. R.; Hush, N. S. Analytic Solutions to Resonant and Non-Resonant Through-Bridge Electronic Coupling. *Nanotechnology* **1996**, *7*, 417–423.
38. Sun, L.; Diaz-Fernandez, Y. A.; Gschneidtner, T. A.; Westerlund, F.; Lara-Avila, S.; Moth-Poulsen, K. Single-Molecule Electronics: from Chemical Design to Functional Devices. *Chem. Soc. Rev.* **2014**, *43*, 7378–7411.
39. McCreery, R. L.; Bergren, A. J. Progress with Molecular Electronic Junctions: Meeting Experimental Challenges in Design and Fabrication. *Adv. Mater.* **2009**, *21*, 4303–4322.
40. Kondo, M.; Tada, M.; Yoshizawa, K. Wire-Length Dependence of the Conductance of Oligo(p-Phenylene) Dithiolate Wires: A Consideration from Molecular Orbitals. *J. Phys. Chem. A* **2004**, *108*, 9143–9149.
41. Wang, G.; Kim, T.-W.; Jang, Y. H.; Lee, T. Effects of Metal−Molecule Contact and Molecular Structure on Molecular Electronic Conduction in Nonresonant Tunneling Regime: Alkyl *versus* Conjugated Molecules. *J. Phys. Chem. C* **2008**, *112*, 13010–13016.
42. Venkataraman, L.; Klare, J. E.; Tam, I. W.; Nuckolls, C.; Hybertsen, M. S.; Steigerwald, M. L. Single-Molecule

Circuits with Well-Defined Molecular Conductance. *Nano Lett.* **2006**, *6*, 458–462.
43. Chen, F.; Li, X. L.; Hihath, J.; Huang, Z. F.; Tao, N. J. Effect of Anchoring Groups on Single-Molecule Conductance: Comparative Study of Thiol-, Amine-, and Carboxylic-Acid-Terminated Molecules. *J. Am. Chem. Soc.* **2006**, *128*, 15874–15881.
44. Kiguchi, M.; Takahashi, T.; Takahashi, Y.; Yamauchi, Y.; Murase, T.; Fujita, M.; Tada, T.; Watanabe, S. Electron Transport through Single Molecules Comprising Aromatic Stacks Enclosed in Self-Assembled Cages. *Angew. Chem., Int. Ed.* **2011**, *50*, 5708–5711.
45. Schneebeli, S.; Kamenetska, M.; Cheng, Z.; Skouta, R.; Friesner, R. A.; Venkataraman, L.; Breslow, R. Single-Molecule Conductance through Multiple $\pi-\pi$-Stacked Benzene Rings Determined with Direct Electrode-to-Benzene Ring Connections. *J. Am. Chem. Soc.* **2011**, *133*, 2136–2139.
46. Kiguchi, M.; Inatomi, J.; Takahashi, Y.; Tanaka, R.; Osuga, T.; Murase, T.; Fujita, M.; Tada, T.; Watanabe, S. Highly Conductive [3 × n] Gold-Ion Clusters Enclosed within Self-Assembled Cages. *Angew. Chem., Int. Ed.* **2013**, *52*, 6202–6205.
47. Chen, I-W. P.; Fu, M.-D.; Tseng, W.-H.; Yu, J.-Y.; Wu, S.-H.; Ku, C.-J.; Chen, C.-h.; Peng, S.-M. Conductance and Stochastic Switching of Ligand-Supported Linear Chains of Metal Atoms. *Angew. Chem., Int. Ed.* **2006**, *45*, 5814–5818.
48. He, J.; Chen, F.; Li, J.; Sankey, O. F.; Terazono, Y.; Herrero, C.; Gust, D.; Moore, T. A.; Moore, A. L.; Lindsay, S. M. Electronic Decay Constant of Carotenoid Polyenes from Single-Molecule Measurements. *J. Am. Chem. Soc.* **2005**, *127*, 1384–1385.
49. Visoly-Fisher, I.; Daie, K.; Terazono, Y.; Herrero, C.; Fungo, F.; Otero, L.; Durantini, E.; Silber, J. J.; Sereno, L.; Gust, D.; et al. Conductance of a Biomolecular Wire. *Proc. Natl. Acad. Sci. U. S. A.* **2006**, *103*, 8686–8690.
50. Wang, C.; Batsanov, A. S.; Bryce, M. R.; Martín, S.; Nichols, R. J.; Higgins, S. J.; García-Suárez, V. M.; Lambert, C. J. Oligoyne Single Molecule Wires. *J. Am. Chem. Soc.* **2009**, *131*, 15647–15654.
51. Moreno-García, P.; Gulcur, M.; Manrique, D. Z.; Pope, T.; Hong, W.; Kaliginedi, V.; Huang, C.; Batsanov, A. S.; Bryce, M. R.; Lambert, C.; et al. Single-Molecule Conductance of Functionalized Oligoynes: Length Dependence and Junction Evolution. *J. Am. Chem. Soc.* **2013**, *135*, 12228–12240.
52. Beebe, J. M.; Kim, B.; Gadzuk, J. W.; Frisbie, C. D.; Kushmerick, J. G. Transition from Direct Tunneling to Field Emission in Metal-Molecule-Metal Junctions. *Phys. Rev. Lett.* **2006**, *97*, 026801.
53. Kim, B.; Beebe, J. M.; Jun, Y.; Zhu, X. Y.; Frisbie, C. D. Correlation between HOMO Alignment and Contact Resistance in Molecular Junctions: Aromatic Thiols *versus* Aromatic Isocyanides. *J. Am. Chem. Soc.* **2006**, *128*, 4970–4971.
54. Yamada, R.; Kumazawa, H.; Noutoshi, T.; Tanaka, S.; Tada, H. Electrical Conductance of Oligothiophene Molecular Wires. *Nano Lett.* **2008**, *8*, 1237–1240.
55. Sedghi, G.; Sawada, K.; Esdaile, L. J.; Hoffmann, M.; Anderson, H. L.; Bethell, D.; Haiss, W.; Higgins, S. J.; Nichols, R. J. Single Molecule Conductance of Porphyrin Wires with Ultralow Attenuation. *J. Am. Chem. Soc.* **2008**, *130*, 8582–8583.
56. Ishida, T.; Mizutani, W.; Aya, Y.; Ogiso, H.; Sasaki, S.; Tokumoto, H. Electrical Conduction of Conjugated Molecular SAMs Studied by Conductive Atomic Force Microscopy. *J. Phys. Chem. B* **2002**, *106*, 5886–5892.
57. Choi, S. H.; Kim, B.; Frisbie, C. D. Electrical Resistance of Long Conjugated Molecular Wires. *Science* **2008**, *320*, 1482–1486.
58. Koch, M.; Ample, F.; Joachim, C.; Grill, L. Voltage-Dependent Conductance of a Single Graphene Nanoribbon. *Nat. Nanotechnol.* **2012**, *7*, 713–717.
59. Huang, M.-J.; Hsu, L.-Y.; Fu, M.-D.; Chuang, S.-T.; Tien, F.-W.; Chen, C.-h. Conductance of Tailored Molecular Segments: A Rudimentary Assessment by Landauer Formulation. *J. Am. Chem. Soc.* **2014**, *136*, 1832–1841.
60. Salomon, A.; Cahen, D.; Lindsay, S.; Tomfohr, J.; Engelkes, V. B.; Frisbie, D. Comparison of Electronic Transport Measurements on Organic Molecules. *Adv. Mater.* **2003**, *15*, 1881–1890.
61. Kolivoška, V.; Valášek, M.; Gál, M.; Sokolová, R.; Bulíčková, J.; Pospíšil, L.; Mészáros, G.; Hromadová, M. Single-Molecule Conductance in a Series of Extended Viologen Molecules. *J. Phys. Chem. Lett.* **2013**, *4*, 589–595.
62. Tada, T.; Yoshizawa, K. Reverse Exponential Decay of Electrical Transmission in Nanosized Graphite Sheets. *J. Phys. Chem. B* **2004**, *108*, 7565–7572.
63. Engelkes, V. B.; Beebe, J. M.; Frisbie, C. D. Length-Dependent Transport in Molecular Junctions Based on SAMs of Alkanethiols and Alkanedithiols: Effect of Metal Work Function and Applied Bias on Tunneling Efficiency and Contact Resistance. *J. Am. Chem. Soc.* **2004**, *126*, 14287–14296.
64. Venkataraman, L.; Klare, J. E.; Nuckolls, C.; Hybertsen, M. S.; Steigerwald, M. L. Dependence of Single-Molecule Junction Conductance on Molecular Conformation. *Nature* **2006**, *442*, 904–907.
65. Onipko, A.; Klymenko, Y.; Malysheva, L.; Stafström, S. Tunneling across Molecular Wires: an Analytical Exactly Solvable Model. *Solid State Commun.* **1998**, *108*, 555–559.
66. Joachim, C.; Magoga, M. The Effective Mass of an Electron When Tunneling through a Molecular Wire. *Chem. Phys.* **2002**, *281*, 347–352.
67. Kohn, W. Analytic Properties of Bloch Waves and Wannier Functions. *Phys. Rev.* **1959**, *115*, 809.
68. Stuyver, T.; Fias, S.; De Proft, F.; Geerlings, P. The Relation between Delocalization, Long Bond Order Structure Count and Transmission: An Application to Molecular Wires. *Chem. Phys. Lett.* **2015**, *630*, 51–56.
69. Xue, Y.; Datta, S.; Ratner, M. Charge Transfer and "Band Lineup" in Molecular Electronic Devices: A Chemical and Numerical Interpretation. *J. Chem. Phys.* **2001**, *115*, 4292–4299.
70. Tsuji, Y.; Hoffmann, R. Frontier Orbital Control of Molecular Conductance and its Switching. *Angew. Chem., Int. Ed.* **2014**, *53*, 4093–4097.
71. Tsuji, Y.; Hoffmann, R.; Movassagh, R.; Datta, S. Quantum Interference in Polyenes. *J. Chem. Phys.* **2014**, *141*, 224311.
72. Movassagh, R.; Strang, G.; Tsuji, Y.; Hoffmann, R. The Green's Function for the Hückel (Tight Binding) Model. *e-print arXiv* **2015**, *1407*, 4780.
73. Li, J.; Tomfohr, J. K.; Sankey, O. F. Theoretical Study of Carotene as a Molecular Wire. *Phys. E* **2003**, *19*, 133–138.
74. Kushmerick, J. G.; Holt, D. B.; Pollack, S. K.; Ratner, M. A.; Yang, J. C.; Schull, T. L.; Naciri, J.; Moore, M. H.; Shashidhar, R. Effect of Bond-Length Alternation in Molecular Wires. *J. Am. Chem. Soc.* **2002**, *124*, 10654–10655.
75. Al-Backri, A.; Zólyomi, V.; Lambert, C. J. Electronic Properties of Linear Carbon Chains: Resolving the Controversy. *J. Chem. Phys.* **2014**, *140*, 104306.
76. Peierls, R. E. *Quantum Theory of Solids*; Oxford University Press: London, 1955.
77. Longuet-Higgins, H. C.; Salem, L. The Alternation of Bond Lengths in Long Conjugated Chain Molecules. *Proc. R. Soc. London, Ser. A* **1959**, *251*, 172–185.
78. Ye, Y.; Zhang, M.; Zhao, J. Ab Initio Investigations on Three Isomers of Polyacetylene under the Interaction of the External Electric Field. *J. Mol. Struct.: THEOCHEM* **2007**, *822*, 12–20.
79. Hudson, B. S.; Kohler, B. E. Polyene spectroscopy: The Lowest Energy Excited Singlet State of Diphenyloctatetraene and Other Linear Polyenes. *J. Chem. Phys.* **1973**, *59*, 4984–5002.
80. Battacharyya, S.; Kibel, A.; Kodis, G.; Liddell, P. A.; Gervaldo, M.; Gust, D.; Lindsay, S. Optical Modulation of Molecular Conductance. *Nano Lett.* **2011**, *11*, 2709–2714.
81. Mulliken, R. S. Quelques Aspects de la Théorie des Orbitales Moléculaires Part V. *J. Chim. Phys.* **1949**, *46*, 675–713.

82. Mulliken, R. S.; Rieke, C. A.; Orloff, D.; Orloff, H. Formulas and Numerical Tables for Overlap Integrals. *J. Chem. Phys.* **1949**, *17*, 1248–1267.
83. Linden, A.; Bürgi, B.; Eugster, C. H. Confirmation of the Structures of Lutein and Zeaxanthin. *Helv. Chim. Acta* **2004**, *87*, 1254–1269.
84. Bartalucci, G.; Coppin, J.; Fisher, S.; Hall, G.; Helliwell, J. R.; Helliwell, M.; Liaaen-Jensen, S. Unravelling the Chemical Basis of the Bathochromic Shift in the Lobster Carapace; New Crystal Structures of Unbound Astaxanthin, Canthaxanthin and Zeaxanthin. *Acta Crystallogr., Sect. B: Struct. Sci.* **2007**, *B63*, 328–337.
85. Helliwell, M.; Liaaen-Jensen, S.; Wilkinson, J. Two Polymorphs of 20-Desmethyl-β-Carotene. *Acta Crystallogr., Sect. C: Cryst. Struct. Commun.* **2008**, *C64*, o252–o256.
86. Bartalucci, G.; Fisher, S.; Helliwell, J. R.; Helliwell, M.; Liaaen-Jensen, S.; Warren, J. E.; Wilkinson, J. X-Ray Crystal Structures of Diacetates of 6-s-cis and 6-s-trans Astaxanthin and of 7,8-Didehydroastaxanthin and 7,8,7′,8′-Tetradehydroastaxanthin: Comparison with Free and Protein-Bound Astaxanthins. *Acta Crystallogr., Sect. B: Struct. Sci.* **2009**, *B65*, 238–247.
87. Note that our closed expression for the Green's function elements does not allow the degree of bond alternation to vary along a polyene chain. Such variation, albeit small in magnitude, does occur. One would include the variable bond distance alternation in any full calculation of the transmission.
88. Dell, E. J.; Capozzi, B.; Xia, J.; Venkataraman, L.; Campos, L. M. Molecular Length Dictates the Nature of Charge Carriers in Single-Molecule Junctions of Oxidized Oligothiophenes. *Nat. Chem.* **2015**, *7*, 209–214.
89. Longuet-Higgins, H. C.; Salem, L. The Alternation of Bond Lengths in Large Conjugated Molecules. III. The Cyclic Polyenes C18H18, C24H24 and C30H30. *Proc. R. Soc. London, Ser. A* **1960**, *257*, 445–456.
90. Wannere, C. S.; Sattelmeyer, K. W.; Schaefer, H. F.; Schleyer, P. v. R. Aromaticity: The Alternating C−C Bond Length Structures of [14]-, [18]-, and [22]Annulene. *Angew. Chem., Int. Ed.* **2004**, *43*, 4200–4206.
91. Solomon, G. C.; Bergfield, J. P.; Stafford, C. A.; Ratner, M. A. When "Small" Terms Matter: Coupled Interference Features in the Transport Properties of Cross-Conjugated Molecules. *Beilstein J. Nanotechnol.* **2011**, *2*, 862–871.
92. Li, Z.; Smeu, M.; Ratner, M. A.; Borguet, E. Effect of Anchoring Groups on Single Molecule Charge Transport through Porphyrins. *J. Phys. Chem. C* **2013**, *117*, 14890–14898.
93. Ulman, A. Formation and Structure of Self-Assembled Monolayers. *Chem. Rev.* **1996**, *96*, 1533–1554.
94. Frisch, M. J.; Trucks, G. W.; Schlegel, H. B.; Scuseria, G. E.; Robb, M. A.; Cheeseman, J. R.; Scalmani, G.; Barone, V.; Mennucci, B.; Petersson, G. A.; et al. *Gaussian 09*, Revision D.01; Gaussian, Inc.: Wallingford, CT, 2009.
95. Schlicke, H.; Herrmann, C. Controlling Molecular Conductance: Switching Off π Sites through Protonation. *ChemPhysChem* **2014**, *15*, 4011–4018.
96. Herrmann, C.; Solomon, G. C.; Subotnik, J. E.; Mujica, V.; Ratner, M. A. Ghost Transmission: How Large Basis Sets Can Make Electron Transport Calculations Worse. *J. Chem. Phys.* **2010**, *132*, 024103.
97. Herrmann, C.; Solomon, G. C.; Ratner, M. A. Local Pathways in Coherent Electron Transport through Iron Porphyrin Complexes: A Challenge for First-Principles Transport Calculations. *J. Phys. Chem. C* **2010**, *114*, 20813–20820.
98. Herrmann, C.; Gross, L.; Steenbock, T.; Solomon, G. C. ARTAIOS—a Transport Code for Postprocessing Quantum Chemical Electronic Structure Calculations. In *Technical Report*; Northwestern University: Evanston, 2010.
99. Todorov, T. N. Tight-Binding Simulation of Current-Carrying Nanostructures. *J. Phys.: Condens. Matter* **2002**, *14*, 3049–3084.
100. Pecchia, A.; Carlo, A. D. Atomistic Theory of Transport in Organic and Inorganic Nanostructures. *Rep. Prog. Phys.* **2004**, *67*, 1497–1561.
101. Solomon, G. C.; Herrmann, C.; Hansen, T.; Mujica, V.; Ratner, M. A. Exploring Local Currents in Molecular Junctions. *Nat. Chem.* **2010**, *2*, 223–228.
102. Gingras, M.; Félix, G.; Peresutti, R. One Hundred Years of Helicene Chemistry. Part 2: Stereoselective Syntheses and Chiral Separations of Carbohelicenes. *Chem. Soc. Rev.* **2013**, *42*, 1007–1050.
103. Milde, B.; Leibeling, M.; Pawliczek, M.; Grunenberg, J.; Jones, P. G.; Werz, D. B. π-Helicenes Truncated to a Minimum: Access Through a Domino Approach Involving Multiple Carbopalladations and a Stille Coupling. *Angew. Chem., Int. Ed.* **2015**, *54*, 1331–1335.